Factors associated with myocardial SARS-CoV-2 infection, myocarditis, and cardiac inflammation in patients with COVID-19

Mayara Bearse , Yin P Hung , Aram J Krauson , Liana Bonanno , Baris Boyraz , Cynthia K Harris , T Leif Helland , Caroline F Hilburn , Bailey Hutchison , Soma Jobbagy , Michael S Marshall , Daniel J Shepherd , Julian A Villalba , Isabela Delfino, Javier Mendez-Pena, Ivan Chebib , Christopher Newton-Cheh , James R Stone

Mod Pathol. 2021 Jul;34(7):1345-1357. doi: 10.1038/s41379-021-00790-1. Epub 2021 Mar 17.

要旨

COVID-19 は、心筋の損傷や機能障害と関連している。致死的な COVID-19 患者では，心筋の炎症細胞浸潤と筋細胞傷害を伴う心筋炎の両方が報告されている。本研究の目的は，COVID-19 で死亡した患者の心臓病理学的変化と SARS-CoV-2 による心臓感染，検査値，臨床的特徴，および治療との関係を明らかにすることである. 後方視的研究において，致死性 COVID-19 患者の連続剖検 41 例を対象に，心臓炎症，心筋炎，SARS-CoV-2 による心臓感染，臨床的特徴，検査値，および治療との関連性を解析した. 心臓感染は in situ hybridazation と NanoString transcriptomic profiling によって評価された。SARS-CoV-2 による心臓感染は，心筋炎を伴うウイルス＋（n＝4），心筋炎を伴わないウイルス＋（n＝26），心筋炎を伴わないウイルス-（n＝11）の 30/41 例で見られた. 心筋感染症例では，心筋の SARS-CoV-2+細胞は稀であり，密度の中央値は 1cell/cm2 であった. ウイルス感染症例では，心筋の CD68+マクロファージと CD3+リンパ球の密度が高く，心電図変化も多かった. 心筋炎は，グルココルチコイドを中心とした非生物学的免疫抑制よりも IL-6 阻害薬使用例でより多く見られた. 全体として，SARS-CoV-2 心筋炎は，非生物学的免疫抑制療法を受けた患者でより少なかった.

Take home message

・致死性の COVID-19 患者では SARS-CoV-2 の心臓への感染はよくみられるが、感染細胞は少量であることが多い。

・心臓の SARS-CoV-2 感染例ではマクロファージとリンパ球密度が増加し、心電図変化 (心房細動、心房期外収縮)も多かった。

・ステロイドをはじめとした非生物学的免疫抑制薬は心筋炎および SARS-CoV-2 による心臓感染の発生率の低下と関連している。

抄読者　伊藤　勇馬　令和 4 年 2 月 28 日

Table 1 Baseline patient characteristics.

	Virus+ with myocarditis	Virus+ without myocarditis	Virus- without myocarditis	*P*[a]
n	4	26	11	
Age (years)	60 (55–64)	71 (33–>89)	62 (21–>89)	0.40
Male sex	2 (50)	19 (73)	6 (55)	0.43
BMI (kg/m^2)	33 (29–36)	30 (20–70)	32 (22–60)	0.36
Caucasian ethnicity	4 (100)	16 (62)	3 (27)	0.03
Hypertension	2 (50)	18 (69)	7 (64)	0.74
Diabetes mellitus	2 (50)	9 (35)	3 (27)	0.71
Hyperlipidemia	1 (25)	13 (50)	3 (27)	0.34
History of CAD	0 (0)	2 (8)	0 (0)	0.55
History of autoimmune disease	0 (0)	3 (12)	1 (9)	0.77
Statin	1 (25)	12 (48), *n* = 25	3 (27)	0.41
ACE inhibitor	1 (25)	2 (8), *n* = 25	2 (18)	0.51
Calcium channel blocker	0 (0)	4 (16), *n* = 25	1 (9)	0.62
Beta-blocker	1 (25)	9 (36), *n* = 25	4 (36)	0.91
Aspirin	0 (0)	10 (40), *n* = 25	2 (18)	0.16
History of smoking	2 (67), *n* = 3	13 (50)	4 (40), *n* = 10	0.31

	Virus+ with myocarditis	Virus+ without myocarditis	Virus- without myocarditis	*P*[a]
(current or former)				
Baseline creatinine (mg/dL)	1.1, *n* = 1	1.0 (0.6–1.6), *n* = 19	1.1 (0.8–2.9), *n* = 5	0.74
Baseline BUN (mg/dL)	19, *n* = 1	17 (11–62), *n* = 17	19 (8–27), *n* = 5	0.88

Data are expressed as median (range) or n (%). For each characteristic, the number of patients is indicated when information regarding the characteristic was not available for all of the patients in the group. ACE angiotensin-converting enzyme, BMI body mass index, BUN blood urea nitrogen, CAD coronary artery disease. a $\chi 2$ or Kruskal–Wallis

Table 2 Autopsy findings.

	Virus+ with myocarditis	Virus+ without myocarditis	Virus- without myocarditis	*P*[a]
n	4	26	11	
SARS-CoV-2+ (cells/cm^2)	1.2 (0.5–3.0)	1.2 (0.4–7.4)	0.2 (0.0–0.3)	<0.001
CD61+ microthrombi present	1 (25)	4 (15)	0 (0)	0.30
Right ventricular strain injury	0 (0)	3 (12)	2 (18)	0.63
Focal isolated pericarditis	2 (50)	6 (23)	1 (9)	0.23

	Virus+ with myocarditis	Virus+ without myocarditis	Virus- without myocarditis	*P*[a]
Postmortem interval (h)	20 (16–26)	20 (4–190)	26 (9–96)	0.82
Heart weight (g)	593 (480–627), *n* = 3	449 (204–646)	480 (267–738)	0.24
Heart weight/upper limit of normal	1.25 (1.04–1.53), *n* = 3	1.02 (0.48–1.67)	1.18 (0.72–1.86)	0.26
Severe coronary artery disease	1 (25)	5 (19)	3 (27)	0.85
Transthyretin amyloidosis	0 (0)	3 (12)	0 (0)	0.39
Composite risk factor score	4.0 (2–6)	4.5 (0–6)	4.0 (1–6)	0.93
Immediate cause of death due to pneumonia/diffuse alveolar damage	3 (75)	23 (88)	9 (82)	0.72
Other immediate causes of death	RP bleed, *n* = 1	Refractory VT, *n* = 1 Acute HF, *n* = 1 PE, *n* = 1	Abdominal organ ischemia, *n* = 2	

Data are expressed as median (range) or n (%). For each characteristic, the number of patients is indicated when information regarding the characteristic was not available for all of the patients in the group. HF heart failure, PE pulmonary embolism, RP retroperitoneal, VT ventricular tachycardia. a $\chi 2$ or Kruskal–Wallis

Fig. 1: Histology of the three pathologically defined patient groups.

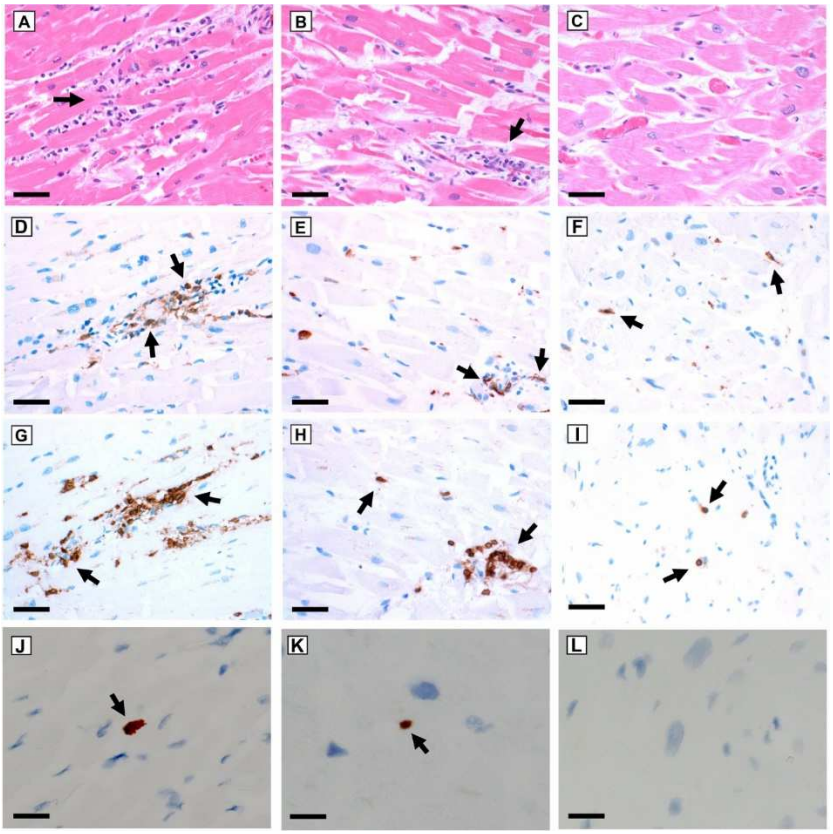

Fig. 1 Histology of the three pathologically defined patient groups. Depicted are histologic images of slides stained with H&E (A–C), immunohistochemistry for the macrophages marker CD68 (D–F), immunohistochemistry for the T-lymphocyte marker CD3 (G–I), and in situ hybridization for SARS-CoV-2 (J–L) for cases with myocarditis along with SARS-CoV-2+ cells in the myocardium (V+M+, A, D, G, J), negative for myocarditis but with SARS-CoV-2+ cells in the myocardium (V+M– , B, E, H, K), and negative for both myocarditis and myocardial SARS-CoV-2+ cells (V– M– , C, F, I, L). There is inflammation with myocardial injury (arrow) in the V+M+ case (A) compared with inflammation (arrow) without injury in the V+M– case (B). Arrows indicate CD68+ macrophages (D–F), CD3+ lymphocytes (G–I), and SARS-CoV-2+ cells (J, K). Scale bars represent 40 μm (A– I) and 80 μm (J–L)

Fig. 2: Transcriptomic assessment of SARS-CoV-2 RNA levels and ACE2 mRNA levels.

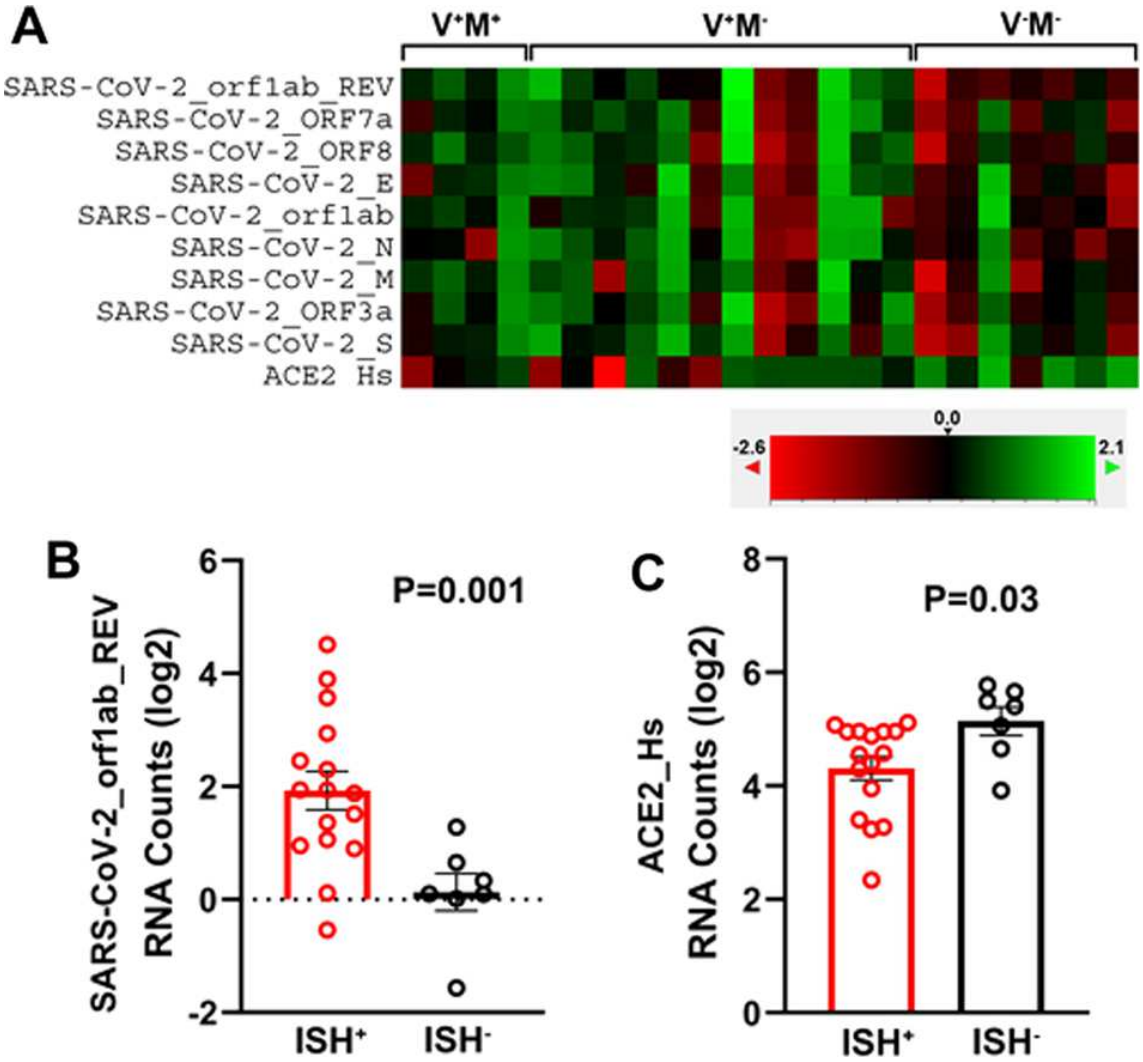

Fig. 2 Transcriptomic assessment of SARS-CoV-2 RNA levels and ACE2 mRNA levels. A heatmap of RNA levels (A) shows trends toward increased SARS-CoV-2-positive-strand RNA transcripts in the SARS-CoV-2-ISH+ cases (P = 0.04–0.29). The color guide shows the corresponding Z-scores for the RNA levels. One V– M– case had relatively strong expression of the eight positive-strand sequences but not the antisense sequence (SARS-CoV-2_orf1ab_REV) likely due to non-replicating virions in the blood. In the SARS-CoV-2-ISH+ cases, there was significantly more SARS-CoV-2 antisense RNA, indicating viral replication in the heart (B), as well as downregulation of the SARS-CoV-2 receptor ACE2 (C). Bars indicate mean ± SE.

Fig. 3: Myocarditis with eosinophils and giant cells in a patient who died from COVID-19.

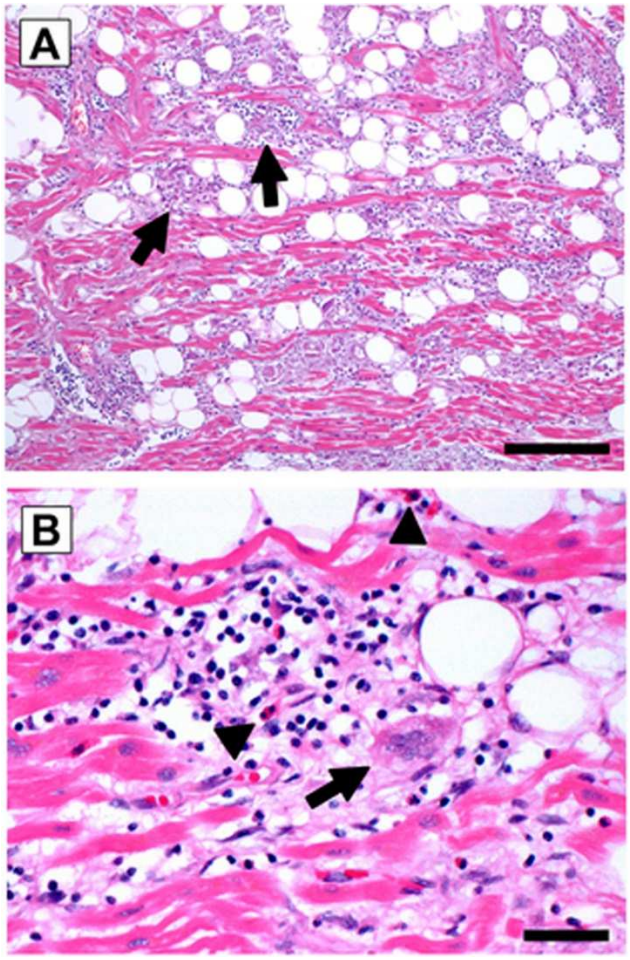

Fig. 3 Myocarditis with eosinophils and giant cells in a patient who died from COVID-19. Depicted are H&E-stained sections. At low power (A), there is diffuse infiltration of the myocardium by inflammation (arrows). At higher magnification (B), both eosinophils (arrow heads) and giant cells (arrow) are identified in the inflammatory infiltrate). Scale bars represent 200 μm (A) and 40 μm (B).

Fig. 4: Associations between myocardial inflammatory cell densities and the presence of myocarditis and cardiac infection by SARS-CoV-2.

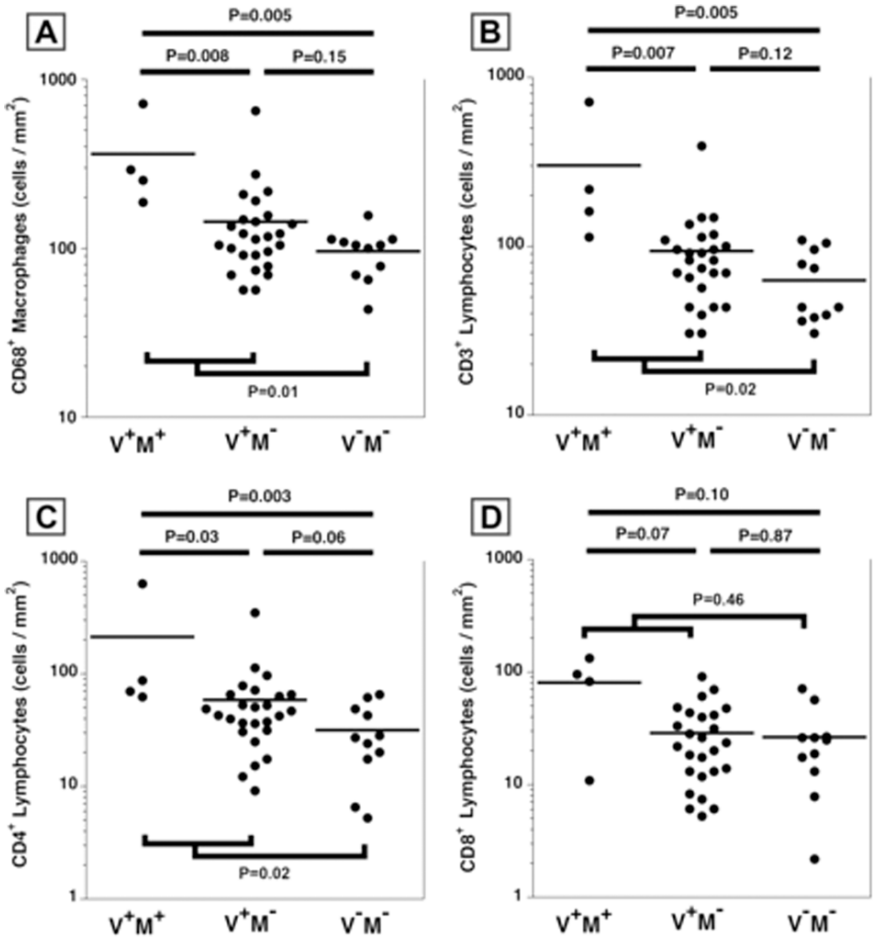

Fig. 4 Associations between myocardial inflammatory cell densities and the presence of myocarditis and cardiac infection by SARS-CoV-2. Depicted are dot plots comparing the densities of CD68+ macrophages (A), CD3+ T-lymphocytes (B), CD4+ helper Tlymphocytes (C), and CD8+ cytotoxic T-lymphocytes (D) between the three pathologically defined patient groups (V+M+, V+M– , and V– M–) as well as the patients with and without cardiac infection by SARSCoV-2 overall. For each cell marker the three groups were first compared using Kruskal–Wallis [P = 0.006 (A), P = 0.005 (B), P = 0.008 (C), P = 0.17 (D)] and then the individual groups were compared using Wilcoxon test.

Fig. 5: Associations of clinical and laboratory features with the pathologically defined patient groups.

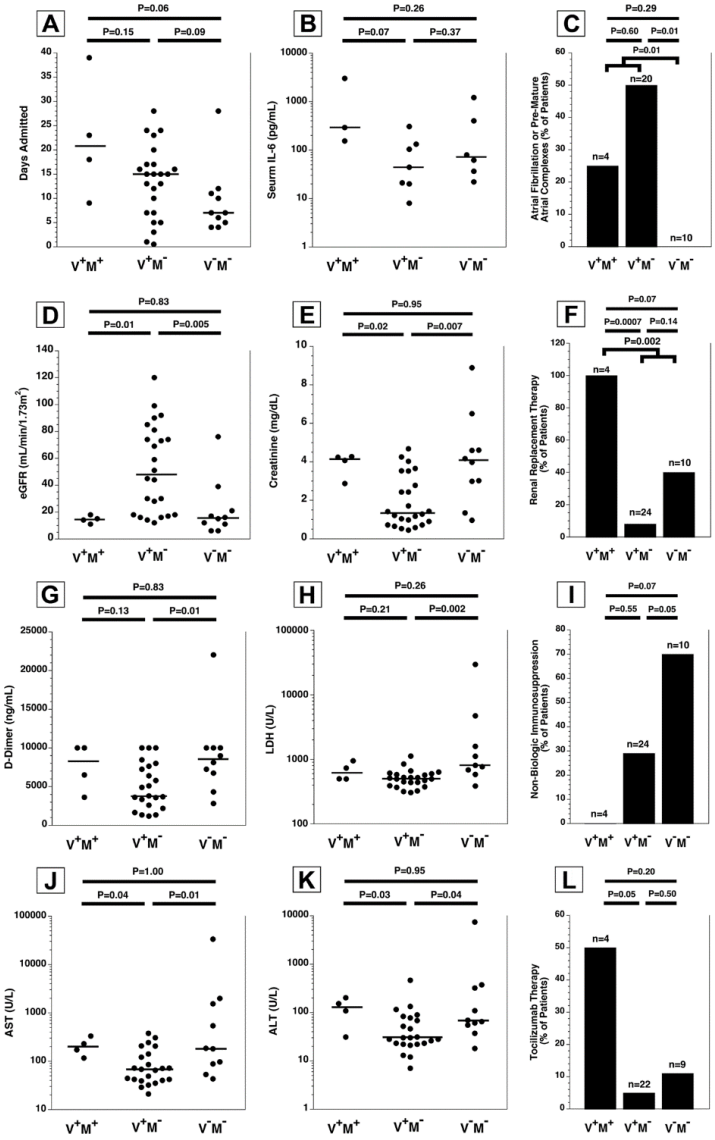

Fig. 5 Associations of clinical and laboratory features with the pathologically defined patient groups. Depicted are dot plots (A, B, D, E, G, H, J, K) and bar graphs (C, F, I, L) comparing selected clinical and laboratory features between the three pathologically defined patient groups. For each cell marker the three groups were first compared using Kruskal–Wallis [P = 0.06 (A), P = 0.12 (B), P = 0.002 (D), P = 0.004 (E), P = 0.03 (G), P = 0.006 (H), P = 0.01 (J), P = 0.03 (K)] or $\chi 2$ [P = 0.02 (C), P = 0.0003 (F), P = 0.02 (I), P = 0.03 (L)], and then the individual groups were compared using either Wilcoxon test or Fisher test.

Fig. 6: Relationships between clinical and laboratory features and myocardial inflammatory cell densities.

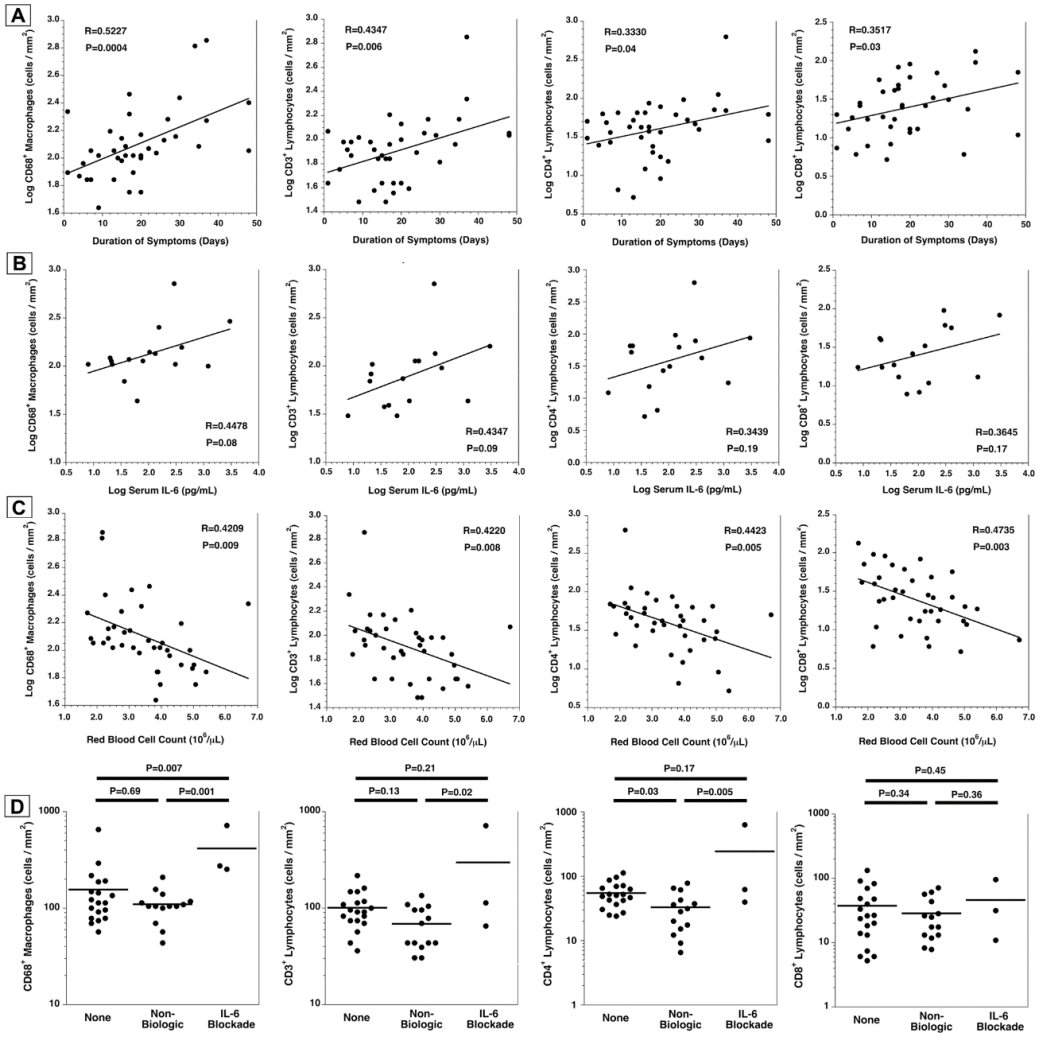

Fig. 6 Relationships between clinical and laboratory features and myocardial inflammatory cell densities. The densities of myocardial CD68+ macrophages, CD3+ T-lymphocytes, and CD8+ cytotoxic T-lymphocytes were all correlated with the duration of hospitalization, and there was a non-significant correlative association between the density of CD4+ helper T-lymphocytes and the duration of symptoms (A). All four inflammatory cell types showed non-significant correlative associations with the serum IL-6 levels (B). All four inflammatory cell types were inversely correlated with the serum red blood cell levels (C). The myocardial inflammatory cell densities were also compared between the patients receiving nonbiologic immunosuppression (see Supplementary Table S2), IL-6 blockade without nonbiologic immunosuppression or no immunosuppression (D). Data were analyzed using linear regression (A, B, C) or ANOVA with post-test by Bonferroni (D).